Trends in Neuroscience

Review

Asymmetry Between Pre- and Postsynaptic Transient Nanodomains Shapes Neuronal Communication

Martin Heine[1],* and David Holcman[2,3],*

Synaptic transmission and plasticity are shaped by the dynamic reorganization of signaling molecules within pre- and postsynaptic compartments. The nanoscale organization of key effector molecules has been revealed by single-particle trajectory (SPT) methods. Interestingly, this nanoscale organization is highly heterogeneous. For example, presynaptic voltage-gated calcium channels (VGCCs) and postsynaptic ligand-gated ion channels such as AMPA receptors (AMPARs) are organized into so-called nanodomains where individual molecules are only transiently trapped. These pre- and postsynaptic nanodomains are characterized by a high density of molecules but differ in their molecular organization and stability within the synaptic membrane. We review the main properties of these nanodomains, as well as the methods developed to extract parameters from SPT experiments. We discuss how such molecular dynamics influences synaptic transmission. The nanoscale organization of active synapses opens new insights into the dynamics and turnover of molecules as well as casting light on their contributions to signal transfer between individual neurons.

Dynamic Nanoscale Organization of Chemical Synapses

Neuronal networks are connected via **chemical synapses** (see Glossary) which constantly change their properties over time, depending on their individual history of activation. The probabilistic nature of synaptic transmission is an inherent property which seems to influence the computational capacity of neurons in the brain [1,2]. The structural and functional mechanisms that maintain flexible synaptic connections between neurons are a key element to guarantee the plasticity of neuronal networks. Interestingly, synapses along individual axons are highly diverse [3] even if they contact the same type of target cells [4,5]. This heterogeneity was proposed to be crucial for the performance of recurrent networks, for example in the CA3 region of the hippocampus [6]. Specifically, the number and diversity of synapses are important for cognitive processes such as retrieval of information, episodic memories, and pattern completion [6,7].

With the advent of super-resolution microscopy that enables the localization of individual molecules, it became possible to explore the subsynaptic organization and resolve the dynamic organization of signaling molecules. In particular, this approach has made it possible to address the fundamental question of how the molecular organization of synapses can ensure two opposite properties: plasticity and stability. In most synapses, the pre- and postsynaptic compartments are composed of an **active zone** (AZ) and a **postsynaptic density** (PSD), respectively. On average, synapses represent patches of 200–500 nm in diameter on the opposing pre- and postsynaptic membranes. These regions contain a finite number of effector molecules such as ion channels and receptors that mediate the signal transduction. A growing body of evidence shows that receptors, voltage-gated ion channels, adhesion molecules, and underlying scaffold

[1]RG Functional Neurobiology, Institute of Developmental Biology and Neurobiology, Johannes-Gutenberg-University Mainz, Hanns-Dieter-Hüsch-Weg 15, D-55128 Mainz, Germany
[2]Data Modeling and Computational Biology Group, Institute for Biology, École Normale Supérieure and Université Paris Sciences et Lettres (PSL Research University), Paris, France
[3]Department of Applied Mathematics and Theoretical Physics (DAMPT) and Churchill College, University of Cambridge, Cambridge CB3 0DS, UK

*Correspondence:
marthein@uni-mainz.de (M. Heine) and
david.holcman@ens.fr (D. Holcman).

proteins are organized into **nanodomains**, as previously predicted from modeling studies [8–10] and that have been confirmed experimentally [11–18]. The number of nanodomains, best investigated for postsynaptic receptor populations, depends on the developmental stage of a synapse and its history of activation [18–20].

In parallel to the nanodomain structural feature, individual receptors, adhesion molecules, and voltage-gated calcium channels can undergo fast displacement to exit or enter a nanodomain. Such displacements are in the range of few tens of nanometers within a time-window of tens of milliseconds, and influence short- and long-term plasticity [13,18,21]. Combining imaging and computational approaches allows quantification of specific parameters of the molecular organization and function of synapses.

In this review we focus on the dynamics of nanodomains, plastic structures that play a central role in sustaining synaptic function. Individual molecular trajectories are used to estimate the properties of these nanodomains: the confinement time of receptors, energy, size, and stability over time that ensure synaptic transmission and plasticity. We describe the pipeline from imaging to data analysis. Note that the molecular organization underlying the presynaptic dynamics of **synaptic vesicles** (SVs), which contributes to synaptic plasticity, was the subject of a recent excellent review [22]. Similarly, the physical laws and stochastic nature of synaptic transmission were recently discussed and reviewed [23–25,48].

Nanodomains Emerge from a Large Volume of Redundant Molecular Trajectories

Revealing the heterogeneity of molecular organization is certainly the most striking achievement of **single-particle trajectory (SPT) analysis** (Box 1 for methods). Segmenting trajectories

Box 1. How Are Nanodomains Visualized and Quantified?

Nanodomains that modulate VGCC positioning have been studied using calcium imaging, calcium buffers (EGTA vs BATPA), and computational modeling. In the context of SPT experiments, several methods have been developed to obtain sufficient numbers of trajectories from individual molecules within a subcellular domain. A key parameter of SPT experiments in addition to the monovalency of the probe is the length of the trajectories, which depends on the properties of the label employed (individual fluorophores, latex beads, or gold particles) and the optical methods used to follow the probe over time. Fluorescence-based approaches are often employed for SPT experiments, either using stochastic conversion of fluorophores (such as mEOS in photoactivation localization microscopy, sptPALM) [40] or stochastic labeling of membrane-associated molecules (as in UPAINT [39]). Both approaches are based on illumination of a reduced probe volume to optimize the spatial resolution of total internal reflection fluorescence (TIRF) microscopy or ultrathin light-sheet microscopy. Moreover, the temporal resolution is limited by the available number of photons from single fluorescent molecules, which limits the length of the trajectories. The collected data do not allow to individual molecules to be directly assigned but generally contain a sufficient number of recurrent events to establish trajectories.

New approaches optimizing the use of available photons from fluorescent probes {e.g., Minflux [100] and interferometric scattering (iSCAT) microscopy of endogenous unlabeled molecular structures [101]} achieve up to 100-fold higher temporal resolution by retaining nanoscale spatial resolution. These methods promise to bring SPT experiments to a spatial and temporal resolution where molecular interactions can be observed in real time.

Once trajectories are collected in the first step, in the next step nanodomains are detected as regions of trajectory accumulation. The main characterizations comprise finding the center, computing the field of velocity, and showing that the trajectories converge at one point. The most difficult part is the detection of the exact location of the boundary, especially for domains of ~80 nm.

The redundancy of trajectories plays a fundamental role in this process by minimizing the effects of noise (instrument noise, localization error, mobility error, etc.) on the geometric features of the well. Small nanodomain boundaries are approximated by a circle or an ellipse. The final step is to compute the energy from trajectories entering the nanodomain. The mean diffusion coefficient is approximated as uniform in such a small domain. Using the diffusion coefficient value and the size of the nanodomain (or potential well), we can estimate the residence time of a trapped molecule, which provides information about the stability of the well for retaining molecules.

Glossary

Active zone (AZ): a region within the presynaptic bouton where SVs are docked and primed before they are released.
AMPA receptors (AMPARs): α-amino-3-hydroxy-5-methyl-4-isoxazolepropionic acid receptors, ionotropic transmembrane receptors for glutamate that are located within the postsynaptic terminal.
Chemical synapses: local contact zones between neurons where signaling molecules are accumulated. Synapses allow neuronal communication by transforming electrical information into neurotransmitter release, which activates postsynaptic receptors. These receptors convert the chemical signal into a local change of membrane potential.
Diffusion: collective motion of Brownian particles generated by thermal noise.
Drift velocity: velocity induced by a deterministic force at a given location.
Energy barrier: energy that must be overcome by a trajectory to escape from a potential well.
Nanocolumn: a multiple alignment of SVs in the presynaptic terminal with a cluster of receptors on the postsynaptic terminal.
Nanodomain: a domain defined as the accumulation of many independent trajectories that indicate a region of high molecular density.
Postsynaptic terminal: the membrane region opposing the presynaptic terminal, and which has an enriched density of receptors that are sensitive to the presynaptic released transmitter.
Postsynaptic density (PSD): a region of high density where receptors are located on the postsynaptic side of a synapse.
Potential well: a bounded high-density region characterized by a deterministic converging field of forces.
Presynaptic terminal: a region on an axon or at the end of an axon where SVs accumulate and where transmitters are released by the opening of VGCCs or by spontaneous SV fusion.
Residence time: the mean time that a trajectory remains inside a nanodomain before escaping.
Single-particle trajectory (SPT) analysis: a method in which individual labeled molecules are followed over time under the microscope. Crucial

(Figure 1A) in confined and unconfined states has confirmed a continuous change in the steady-state organization of individual molecules. Interestingly, confined behavior is a property of the medium itself because it is found in independent overlapping trajectories. This finding demonstrated that the heterogeneous organization of small subcellular compartments can be sampled by the stochastic motion of molecules. Whether the underlying motion is free **diffusion** or a more complex motion pattern has remained an important question that can be addressed by combining the statistical properties of trajectories. One example is the organization of store-operated calcium channels, where the pore-forming subunit (ORAI) in the plasma membrane interacts with the calcium-sensing protein STIM in the membrane of the endoplasmic reticulum (ER) [26]. To form the functional complex, STIM and ORAI molecules aggregate in membrane-membrane contacts which allow channel opening and refilling of intracellular calcium stores. Thus, upon activation, both STIM and ORAI molecules transiently change their diffusion profiles. In addition to their transient confinement, individual dynamics crucially impacts on the speed of complex formation and determines the probability that the STIM and ORAI complexes will meet and interact. More generally, transmembrane molecules such as receptors, adhesion molecules, **voltage-gated calcium channels** (VGCCs), and **SNARE complex** proteins at both sides of the synapse [12,16,27], and postsynaptic **AMPA receptors** (AMPARs) [17], GABA receptors (GABAARs) [28], neuroligin [15], α-neurexin [13,14], VGCCs [29], syntaxin 1A, glycine receptors [30], and NMDA receptors (NMDARs) [18] can form transient nanodomains; this is the central focus of this review.

What Is a Nanodomain?

A nanodomain is defined empirically as a region of few tens to hundreds of nanometers in size where the trajectories of individual molecules are confined and accumulated (Figure 1A and Box 1; see also https://youtu.be/1rdeSzkWBEQ). In synapses, the concept of nanodomain organization was initially introduced to characterize the coupling between calcium channels and SVs during synaptogenesis [31]. The exact physical properties how molecules and particular VGCCs organize into nanodomains are not fully understood. Several mechanisms have been suggested, including long-range effects of scaffold proteins, interactions with cytoskeletal elements, interactions with the extracellular matrix, membrane–membrane contacts, and long-range membrane curvature-induced confinement [32,33]. However, can individual molecular interactions resolve the nature of confinement? Most confined proteins could be forced to stay together by a plurality of contributing elements, and it remains difficult to resolve their contributions: local molecular interactions are effective within a range less than tens of nanometer, and thus cannot explain long-range interactions over hundreds of nanometers. Other contributing mechanisms could involve charged unstructured proteins, membrane curvature, scaffolding organizations, and probably more. Developing a sensitive measure of the strength of a confinement could help in translating these structural features into a physiological context. One approach to quantify the strength of nanodomains has been developed by estimating the field of forces that are hidden in the Brownian behavior of many trajectories. A confined motion can be characterized by a combination of several parameters: local diffusion coefficient, length of confinement, and the **residence time** of a trajectory inside a nanodomain. Note that a reduction of the diffusion coefficient in a nanodomain can be obtained theoretically by increasing the density of impenetrable obstacles [34,35], but cannot be produced by long-range deterministic forces because diffusion is generated by random collision not by deterministic forces.

To identify a nanodomain, a large number of redundant trajectories passing through the same position many times is needed (Figure 1A). In early SPT experiments, single trajectories were analyzed so as to observe individual molecules for as long as possible to generate individual molecule-based information only from non-overlapping trajectories [36–38], from which it was

parameters are label size and stability, as well as the density of individual molecules within the cell membrane. The precision of tracking depends on localization accuracy as well as on the temporal resolution. Most SPT methods (for example sptPALM) compromise between temporal and spatial resolution, leading to a coarse-grained representation of molecular motion over time. Trajectories are reconstructed using a tracking algorithm.

SNARE complex: a molecular complex that mediates docking, priming, and fusion of SVs with the presynaptic membrane.

sptPALM: single-particle tracking photoactivated localization microscopy, a fluorescence microscopy imaging method that allows the detection of SPTs based on the stochastic emission of fluorophores coupled to individual molecules.

Synaptic vesicles (SVs): organelles that are constantly recycled at synapses and that contain neurotransmitters for release during synaptic transmission. SVs fuse to the plasma membrane during neurotransmitter release.

UPAINT: Universal point accumulation for imaging in nanoscale topography, a fluorescence microscopy imaging method that utilizes dynamic imaging of continuously labeled molecules.

Voltage-gated calcium channels (VGCCs): a class of voltage-sensitive channels that are permeable to calcium ions, the key effector ions that trigger SV fusion and neurotransmitter release.

not possible to extract biophysical parameters about the membrane. The collected statistics were correlated to markers for pre- and postsynaptic structures along the trajectories, pooling all information within time-intervals or within a single parameter such as the diffusion coefficient. It was already recognized that the heterogeneity within individual trajectories is probably a function of the location of synaptic molecules. By recording many short trajectories for many molecules using methods such as **sptPALM** or **UPAINT** [39,40], many redundant trajectories were reconstructed (Box 1). These data have made it possible to begin to retrieve the organization of the local environment (cytoplasm, membrane) that is explored by individual molecules.

High-density regions are identified by plotting the density of points irrespectively of the arrow of time [12,13] (Figure 1). In addition to technical issues such as localization accuracy and fluorophore blinking [41], these high-density regions cannot be obtained by simply increasing the density of obstacles, but are further characterized by a converging field of velocity (Figure 1B) [13,27,42,43]. This specific structure suggests that there is a local membrane organization that attracts trajectories at hundreds of nanometers distance and confines them. Indeed, nanodomains are located at strategic positions and correlate with synaptic structures such as the presynaptic AZ and postsynaptic dendritic spines. In the case of inhibitory or excitatory synapses, scaffolding proteins partially contribute to this process [12,27,42], suggesting that several redundant mechanisms contribute to synaptic organization.

A crystal-like organization, as revealed for scaffold proteins in inhibitory synapses [30], could only create nanodomains a few nanometers in size [44]. Thus, to confine molecules at the 100 nanometer scale, a further level of organization is necessary to create long-range forces.

How Are Nanodomains Characterized?

It is not enough to characterize nanodomains as a high density of points. A crucial property for their functional relevance is the force that maintains this structure over time. A **drift velocity**
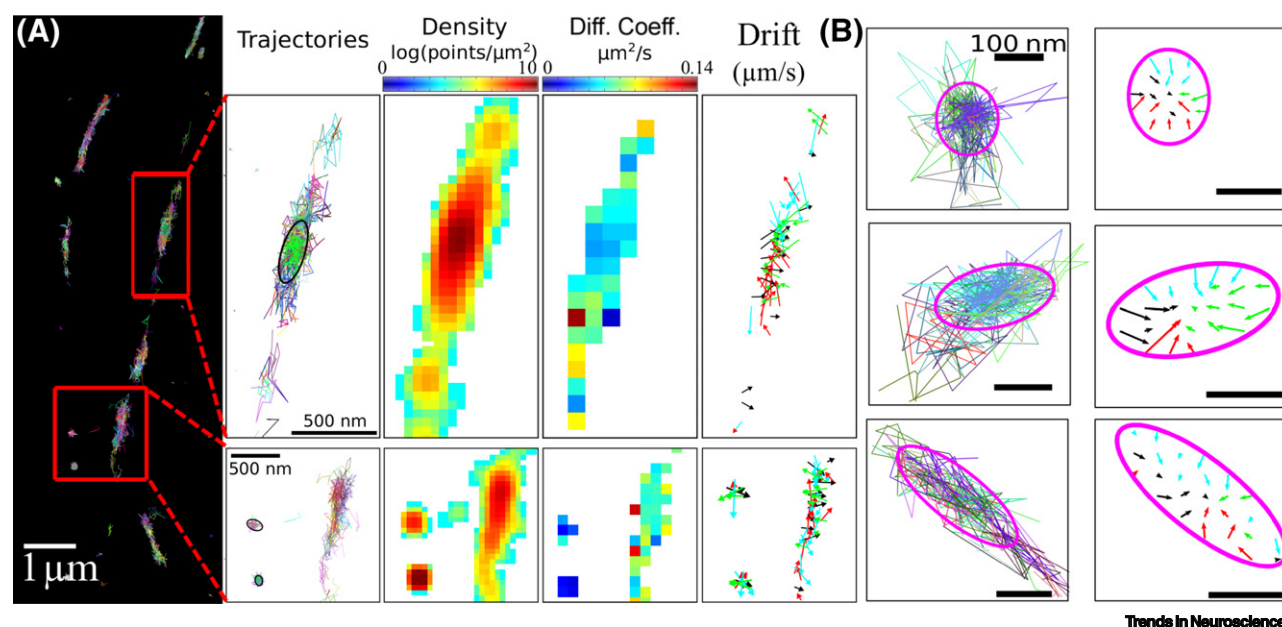
Figure 1. Voltage-Gated Calcium Channel (Ca$_V$) Nanodomains Revealed by Single-Particle Trajectories. (A) Examples of Ca$_V$ trajectories along axons of hippocampal neurons: the two insets show (i) multiple clustered trajectories, (ii) the density of points, (iii) diffusion coefficients (Diff. Coeff.), and (iv) the drift field, indicated by converging arrows. (B) Rows: three nanodomains (high-density regions); left/right: trajectories and vector fields. Figure adapted, with permission, from [13].

analysis revealed a converging arrow with a center where the domain is generally approximated as an ellipse (Figure 1B). However, one major difficulty is to determine the exact boundary [45] and the nature of the motion at the boundary, which could be divided into regions where trajectories are reflected [46].

Once the geometric parameters and the effective diffusion coefficient of a nanodomain have been estimated, it is possible to compute its associated energy in kT (Figure 1C), similar to that of a chemical interaction. This energy characterizes the strength of the well in retaining particles and allows evaluation of how long individual molecules stay within such a nanodomain [34]. Indeed, a classical measure of the stability of a nanodomain is the mean residence or dwell time of a particle inside the domain. This concept was introduced more than 80 years ago and has been developed over decades in the physics literature [44,47]. The escape time from a field of force specifically depends on the energy (potential barrier, the difference of the energy between the boundary and the center of the well), the diffusion coefficient, and the geometry of the domain such as its size. This concept is at the base of chemical physics and has been extended to subcellular nanodomains: for example, the time to escape from a nanodomain with a constant flat **potential well** is given in Equation 1.

$$\bar{\tau} = \sqrt{\frac{2\pi\gamma}{D}} \frac{\pi |\Omega|}{\omega_\perp |\partial\Omega|} e^{E|kT} \qquad [1]$$

where E is the **energy barrier**, k is the Boltzmann constant, T the temperature, γ the viscosity, D the diffusion coefficient, $|\Omega|$ (resp. $|\partial\Omega|$) is the surface (resp. the boundary length) of the nanodomain, and $\omega_\perp$ is a constant that represents the frequency of the potential barrier perpendicular to the boundary [46].

It is also possible that the residence times of individual diffusing molecules are correlated with one another. In that case, the mean escape time is not sufficient to characterize the strength of a given nanodomain because the residence time could now depend on their concentration, as predicted theoretically in [48]. Because the residence time depends on the number, the binding rate, and the time to escape the nanodomain, it could be tempting to determine the residence time by using only the statistics of many single trajectories without any physical models. A problem that arises at this point is that the length of trajectories is in most cases largely insufficient because of photobleaching of the fluorophore, which can lead to underestimation of trajectory length. Hence, the statistics of many short trajectories should be combined in a model to define the location of the boundary of the nanodomain and to evaluate the physical quantities. In summary, a nanodomain is a complex structure that attracts trajectories within hundreds of nanometers. Their analysis reveals the residence time and the strength by which molecules are retained. The energy of a nanodomain measures its stability over time.

Once a nanodomain has been identified, one can also extract its stability over time using a time-lapse analysis (Figure 2A,B) based on overlapping a sliding window of tens of seconds. Only a fraction of trajectories inside the time-window will be used for the statistical analysis and will profit from the recurrent blinking behavior of fluorophores. Provided that there are enough trajectories, the change in the quantities (such as the energy and the morphology of the well) over time reveals how dynamic the nanodomains are (Figure 2C). Using this approach, we have found that nanodomains differ in their stability over time and are able to move and deform [13,27]. For example, VGCC (for short $Ca_V2.1_{\Delta47}$ and long $Ca_V2.1_{+47}$ splice variants) wells remain stable with a mean time of 30 s (Figure 2D).
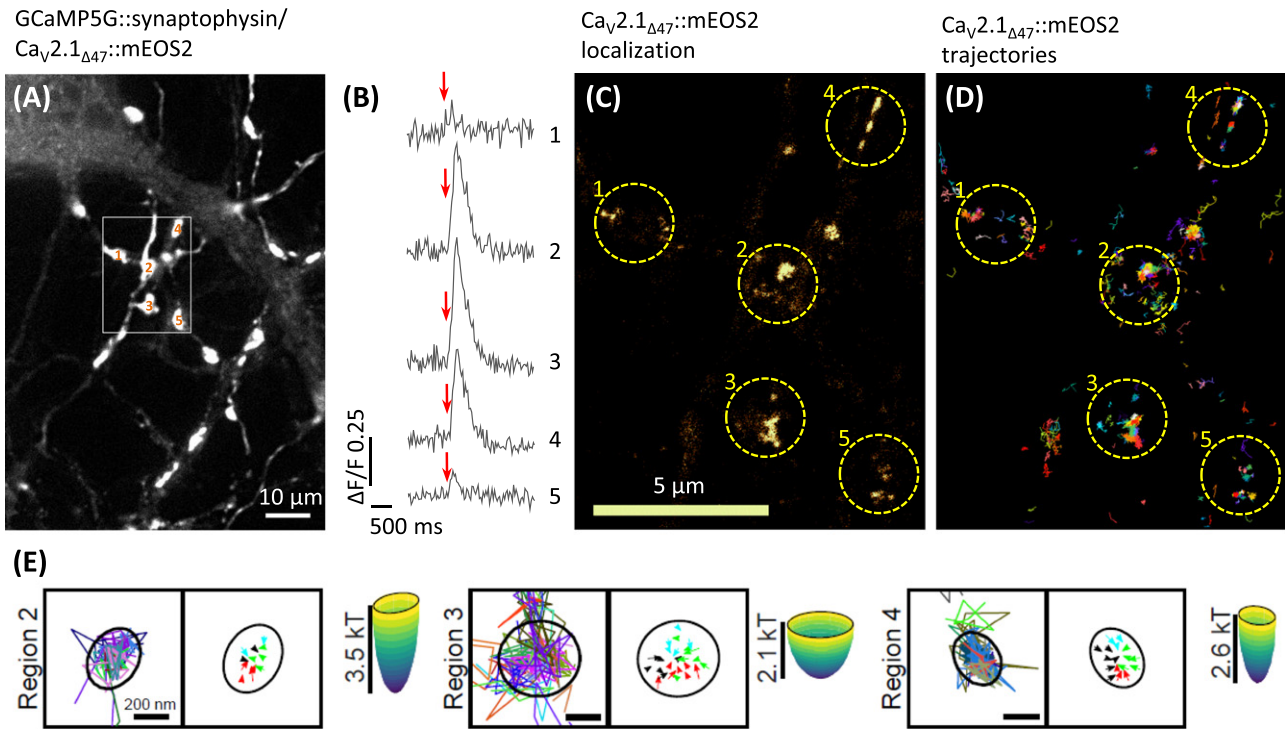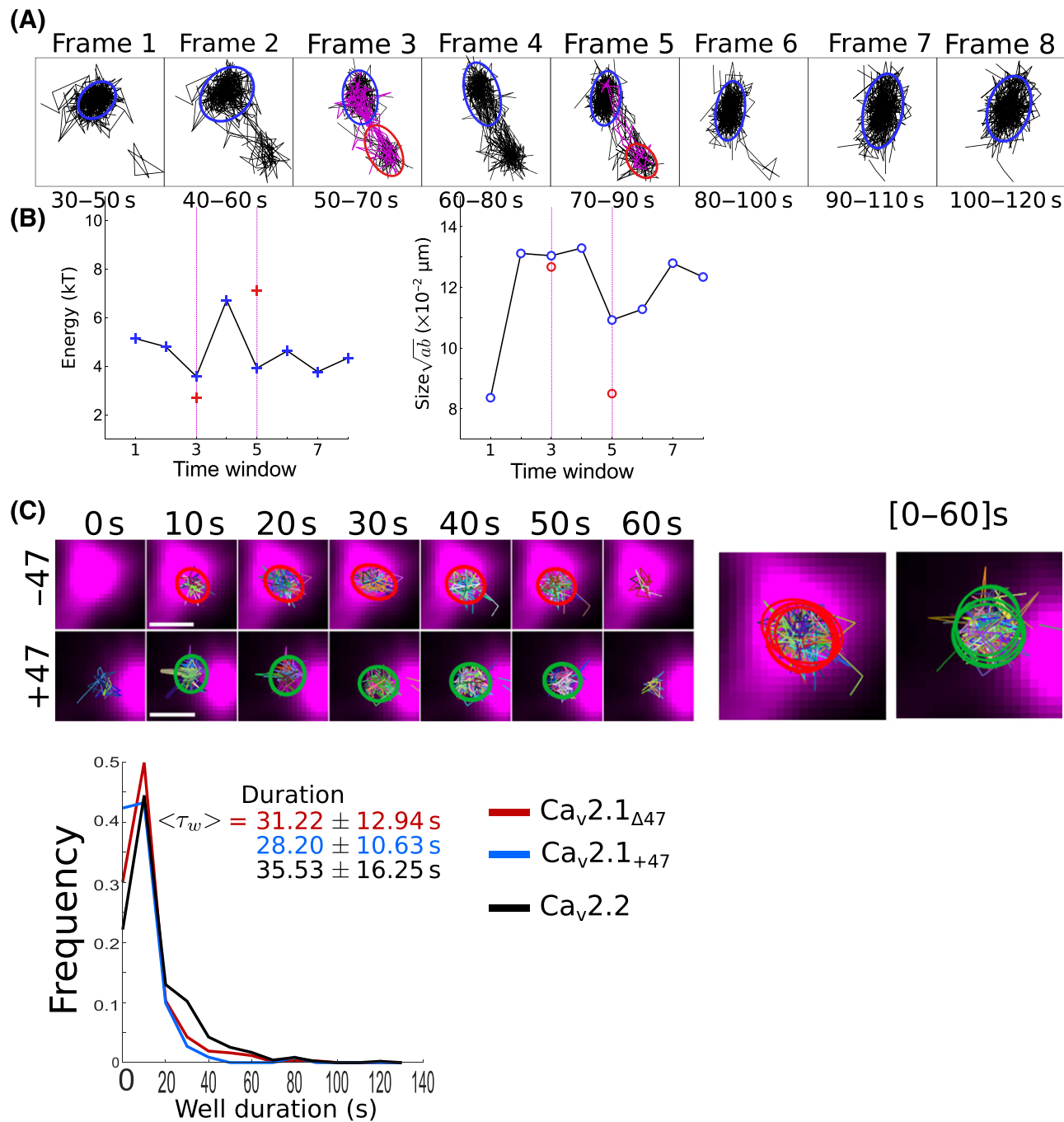
Figure 2. Nanodomains Correlated with Synaptic Calcium Transients. (A) Axonal branches transfected with GCamp::synaptophysin and Ca$_V$2.1$_{\Delta 47}$::mEOS2. (B) Individual presynaptic calcium responses to a brief 4-aminopyridine (4AP)-like stimulus with 50 ms interstimulus interval for selected synaptic boutons in panel A. (C) Localization map of Ca$_V$ trajectories (Ca$_V$2.1$_{\Delta 47}$::mEOS2 molecules) within the indicated region from panel A. (D) Shown are color-coded individual reconnected trajectories of Ca$_V$2.1$_{\Delta 47}$::mEOS2 molecules. (E) Magnified synaptic regions corresponding to the selected synapses. The circle represents wells identified for the three examples and vector fields where arrow lengths are proportional to the velocity. 3D representation of parabolic potential wells and their associated energies in kT. Figure adapted, with permission, from [13].

What Are the Roles of Nanodomains?

The most obvious function of nanodomains is to retain diffusing molecules, for example channels or receptors, at a specific location. They probably maintain a steady-state number of channels or receptors. Another role of nanodomains could be to anchor a fraction of molecules close to their optimal location to achieve a physiological function, as suggested for AMPARs trapped in endocytotic pits, which can be liberated during synaptic plasticity to enter the postsynaptic density [49]. Similar ideas were proposed for clusters of voltage-gated potassium channels (K$_V$2.1 and K$_V$2.2) which contain hundreds of non-conducting channels provided that they are in contact with the ER membrane via VAMP-associated proteins (VAPs). The formation of a K$_V$2.1 cluster is phosphorylation-dependent and conditions such as hypoxia/ischemia lead to liberation of conducting channels from the cluster [50,51]. Hence, transient trapping depends not only on the number of binding partners (e.g., scaffolding molecules) but also on the mechanism of molecular exchange. These confining mechanisms define the average dwell time within nanodomains that can be extracted without precise specification of the interacting partners based on data obtained from super-resolution experiments (sptPALM or UPAINT). Finally, nanodomains induced by VGCC accumulation at synapses (Figure 3A) are associated with local calcium transients (Figure 3B–D) and thus could regulate their amplitude by forcing cooperativity (coactivation of individual channels) within the **presynaptic terminal** [52] or by induction of cooperative gating by calcium-induced channel linking via calmodulin [53].

(A)

Frame 1	Frame 2	Frame 3	Frame 4	Frame 5	Frame 6	Frame 7	Frame 8
30–50 s	40–60 s	50–70 s	60–80 s	70–90 s	80–100 s	90–110 s	100–120 s

(B)

(C)

0 s 10 s 20 s 30 s 40 s 50 s 60 s   [0–60]s

Duration
$\langle \tau_w \rangle = 31.22 \pm 12.94$ s
28.20 ± 10.63 s
35.53 ± 16.25 s

— $Ca_v2.1_{\Delta47}$
— $Ca_v2.1_{+47}$
— $Ca_v2.2$

Figure 3. Transient Nanodomains. (A) Dynamics of wells over time ($Ca_v2.1$ splice variants and $Ca_v2.2$) within the presynaptic membrane. Regions of high density can change shape, drift, and new regions can appear and disappear. (B) Changes in the energy and size (for the two main axes a and b of the ellipse) of potential wells associated with the nanodomains shown in panel A. (C) As in A with a final overlap of the wells for $Ca_v2.1_{\Delta47}$ (green) and $Ca_v2.1_{+47}$ (red). (D) Time distribution of well duration (τ_w) as a measure of their stability. Figure adapted, with permission, from [13].

How Does Nanoscale Confinement of Receptors and Channels Contribute to Synaptic Function?

Are the dynamics of individual molecules relevant for synaptic function? VGCC clustering near SVs was reported to be associated with high release probability, reliable synaptic transmission, and differentiation of temporal information [24,52,54–59]. By contrast, a uniform distribution of VGCCs at a variable distance from SVs is associated with a lower release probability, as well as stochastic and asynchronous release, that define the temporal integration properties of synapses [1,52,58]. Thus VGCC nanodomains (revealed by a high density of trajectories in Figure 3A–D) at synapses could be crucial in maintaining a necessary VGCC density in close proximity to SVs but also to ensure that the calcium influx accumulates and compensates for kinetic properties (steady-state inactivation) of VGCCs. This suggests that there could be a variety of VGCC nanodomains: some allowing VGCCs to move uniformly in the domain whereas other very steep domains (measured by their local energy; Figure 3E) restrict their motion and increase the reliability of transmitter release. To conclude, by changing the size of a VGCC nanodomain, a synapse could modulate the release probability. Thus, it seems obvious that VGCC nanodomains influence the local transient concentration of VGCCs and local calcium transients, and contribute to the heterogeneity of synaptic transmission [60].

Beyond Nanodomains

It is often difficult to obtain an exact characterization of a region explored by SPTs that does not attract SPTs by exerting a deterministic force. Molecules are generally reported to show free Brownian motion. However, there are some exceptions: a persistent drift was reported in a sub-population of spine necks within postsynaptic spines of glutamatergic synapses which could alternate after a few minutes [27]. In addition, an alternating flow was found in tubules of the ER network [61]. For all other cases (in the absence of flow or converging forces), it remains an open question how the dynamics of trajectories is linked to the structural and molecular organization of the membrane. In particular, the organization of a membrane containing impenetrable obstacles cannot generate confined nanodomains but changes the effective diffusion coefficient. The density of obstacles can be estimated from changes in the diffusion coefficient based on many trajectories [34].

Nanodomains in Pre- versus Postsynaptic Terminals

Within synapses, the nanoscale organization of molecules can be directly linked to their function in neuronal activity. However, presynaptic VGCCs and postsynaptic AMPARs show substantial differences in their nanodomain dynamics and the dwell time of individual molecules, as we shall illustrate by two examples.

Nanodomains in the Presynaptic Terminal

There are one or more AZs within the presynaptic membrane of most cortical synapses, and each AZ has several individual release sites that define the number of releasable SVs [62]. The number of release sites ranges from 4 to 15 [22] and the timecourse of SV turnover depends on the action of a complex molecular machinery that sets the temporal boundaries for SV delivery and recycling [25,63–65]. SV fusion depends on the association with the SNARE complex. The plasma membrane-associated SNARE protein syntaxin 1A has been identified to organize in nanodomains which can be altered in their organization and composition by activity [29,66]. The mechanism of formation depends on association of syntaxin 1A with plasma membrane lipids based on hydrophobic and ionic interactions between syntaxin transmembrane domains and lipids [67]. These mechanisms are suitable to prepare for rapid SV release and reassembly during high-frequency synaptic transmission, and thus contribute to dynamic reorganization during synaptic activity [25].

To trigger the release of SVs, the distance between release sites and VGCCs is the predominant variable for the last and fastest step of evoked SV release (0.5–1 ms) [63]. Other parameters such

as the calcium sensitivity of the vesicular calcium sensor, the intracellular calcium buffering capacity, and VGCC kinetic properties modulate the coupling between SV and VGCCs, which has been explored for several synapses [56–58,68–72]. The organization of VGCCs with respect to the release sites is classically investigated by manipulations of available free calcium ions using calcium chelators with different binding properties [73], thus allowing synapses to be classified as being tightly (<20 nm) or loosely (>20 nm) coupled. This means that, for action potential-evoked SV release, only the position of available VGCCs is crucial. The spatial relationship between SVs and calcium channels at the moment of release (which occurs on a timescale of <1 ms) can be considered to be static. However, ~60% of VGCCs localized within the presynaptic membrane have been reported to be mobile [14], and each SV fusion event imposes an addition of membrane material, inducing local reorganization within the AZ. Nevertheless, how do synapses maintain a specific coupling distance between VGCCs and SVs? Constant reorganization of VGCCs as a result of their local dynamics and the position and size of the nanodomains that retain VGCCs are certainly crucial [13,14], but the exact relationship between VGCC nanodomains and SVs remains unclear. How stable are VGCCs in the synaptic membrane during synaptic activity? Within hippocampal synapses, we estimated that ~9 VGCCs could be transiently confined in 1–2 nanodomains and dwell there for a time interval of ~100 ms [13], much longer than triggering SV release from an invading action potential. How can these nanodomains of VGCCs influence SV release? Two models are currently favored. First, the perimeter model implies tight coupling between VGCC clusters that are surrounded by SVs [57]. Second, the exclusion zone model proposes a defined distance of >20 nm between VGCC clusters and SVs [74]. Measurements of the mean number of release sites suggest that 4–10 are present in the AZ of a hippocampal synapse positioned at a mean distance of ~90 nm [22]. This further suggests that each VGCC nanodomain may be coupled to several release sites. The mean dwell time of ~100 ms within a nanodomain, as well as the estimated number of ~9 VGCCs per nanodomain, indicate that a substantial fraction of VGCCs are located outside nanodomains [13]. Hence, nanodomains primarily maintain a critical number of VGCCs to reliably trigger SV release, whereas VGCCs outside nanodomains might instead participate in spontaneous SV release by stochastic opening of the channel or by SV recycling [75–78]. The possibility that VGCCs can enter and leave nanodomains may serve two functions. First, it can equilibrate the fraction of inactivated VGCCs within the nanodomain. Second, it allows the distance between VGCCs and SVs to be modulated to trigger their evoked, spontaneous, or asynchronous release. However, how can such a specific coupling distance between individual VGCCs and SVs be maintained within nanodomains? Reported interactions with scaffold proteins, SNARE proteins, and auxiliary calcium channel subunits ([79,80] for recent reviews) can potentially affect VGCC–SV coupling. However, individual binding sites could define the coupling distance or dwell time of VGCCs within nanodomains. We studied the impact of molecular interactions of VGCCs and scaffold proteins by investigating the organization and functional impact of C-terminal splice variants of the pore-forming VGCC α1 subunit of $Ca_V2.1$ (P/Q-type) channels [13]. This allowed us to probe whether gain or loss of channel–scaffold interaction impacts on the SV release properties of the synapse. Surprisingly, the full-length VGCC C-terminus (expressing additional interaction sites) seems not to tighten the connection between SVs and VGCCs ($Ca_V2.1$) but instead induces an exclusion zone. By contrast, splicing-dependent loss of the distal C-terminus allows the channel to approach closer to SVs closer, as evidenced by a significantly higher release probability at synapses dominated by the short C-terminal splice variant [13].
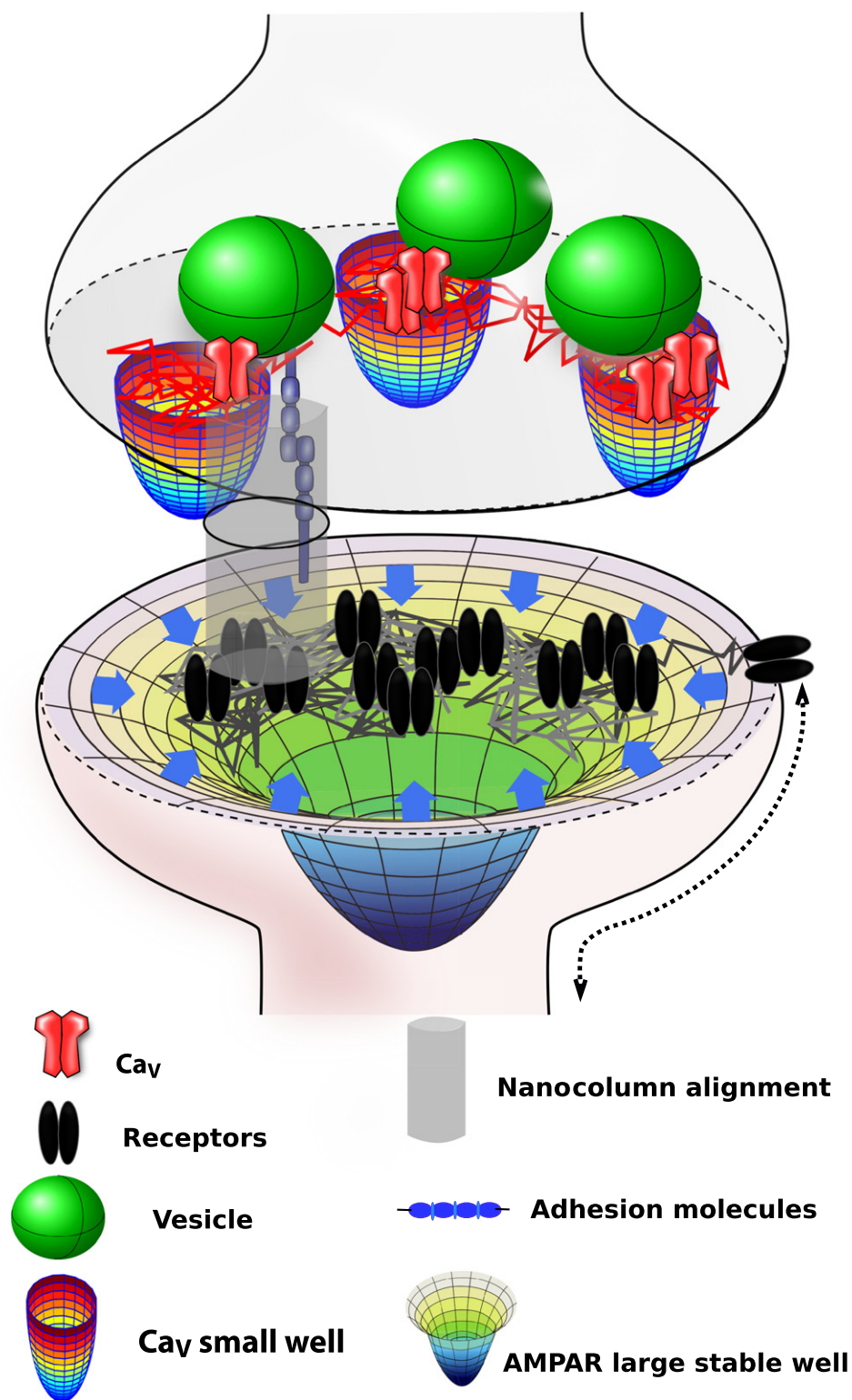
To conclude, the dynamic organization of the AZ allows VGCCs to move between nanodomains. Their contribution to evoked SV release depends on their individual interactions with, for example, scaffold proteins, and hence tunes the probability of SV fusion within a timescale of milliseconds to seconds which has a profound impact on short-term plasticity [13].

Nanodomains in the Postsynaptic Terminal

The presence and function of postsynaptic nanodomains of AMPARs has been reviewed extensively in excellent recent reviews [79,81]. We only briefly recapitulate the description of nanodomains in the postsynapse to compare them with presynaptic organization. Nanodomains in **postsynaptic terminals** were initially described theoretically as trapping potential well regions [46], and later on were confirmed experimentally using SPTs in excitatory [18,27] and inhibitory [42] synapses. The size of these nanodomains was first thought to be about 200–300 nm, a region where AMPARs remain for seconds to minutes [27]. Probing AMPAR nanodomains with several imaging techniques revealed smaller (80–100 nm) but stable (minutes to hours) nanodomains containing about 20 receptors [12]. These smaller nanodomains were detected using the density of points, but not the displacement of trajectories, where temporal causality is crucial to estimate the drift and the energy of the nanodomain. The number of these nanodomains ranges from 1–3 per postsynaptic density and can be changed during synaptic plasticity [19]. The link between these subdomain clusters and potential well-based nanodomains remains to be established. Similar arrangements were found in GABAergic synapses [17]. Postsynaptic nanodomains are localized within the center of the postsynaptic density and are partially dependent on the interaction with underlying scaffold elements. Deleting scaffold components such as PSD95, or scaffold interaction sites located either directly on the AMPAR or on their auxiliary subunits, only partially resolved the clustered organization of AMPARs [82–84], indicating multiple redundant bounds with scaffolds and other proteins within the PSD, relatively similar to the organization of the presynapse. The molecular composition of AMPARs within nanodomains is heterogeneous and most likely synapse-specific, particularly in respect to subunit composition and auxiliary subunits as TARPs, Shisa proteins, and cornichons [85–89] which impact on receptor traffic, PSD interactions, and kinetic properties. Thus, the nanoscale clustering of AMPAR is activity-dependent [90–92] and confirms modeling data on subsynaptic receptor organization and their impact on the synapse performance over time [46,93]. With respect to NMDARs, they also show stochastic motion that is regulated by neuronal activity [20], but the nanodomain organization characterized by electrophysiology, spectrometry, and freeze-fracture immunolabeling showed that the number of NMDARs is independent of PSD size, with a diameter of ~176 nm for the central NMDAR cluster, and it was estimated that there are ~20–30 NMDAR-type structures per PSD. NMDAR nanodomains depend not only on the composition of the receptor complex but also on the developmental state of the synapse [18]. Although the three scaffolds PSD95, PSD93, and SAP 102 are involved in maintaining AMPARs and NMDARs trapped at the PSD, the nature of the nanodomains, their residence time, and a possible potential well-related PSD interaction can also be expected for NMDARs, but has not been yet investigated [94].

The Mean Lifetime of Nanodomains in Pre- and Postsynaptic Terminals Differs Substantially

Although there is large variability in the composition of individual synapses, for an active cortical synapse one might probably find 10–50 VGCCs on the presynaptic side, whereas there are 10–400 AMPARs on the postsynaptic side. In respect to the localization of their nanodomains, nanodomains of VGCCs have also been frequently found outside presynaptic compartments along the axon, whereas dendritic AMPAR-containing nanodomains are almost exclusively localized at synapses and dendritic spines [27]. At postsynaptic terminals, drift-based nanodomains have a radius 200–400 nm, whereas nanodomains in the presynapse are much smaller (~80 nm). The energy of the wells, which characterizes their strength to retain receptors, is 3–6 kT and occasionally >8 kT for AMPARs, whereas it is 3–4 kT for VGCCs. The residence time for AMPARs is a few to several minutes, whereas it is only ~120 ms for VGCCs (~4–5-fold longer than free diffusion). This comparison clearly shows that the postsynaptic population of AMPARs is much more stable than that of presynaptic VGCCs. In addition, AMPAR nanodomains

Ca$_V$

Receptors

Vesicle

Ca$_V$ small well

Nanocolumn alignment

Adhesion molecules

AMPAR large stable well

Trends in Neurosciences

(See figure legend at the bottom of the next page.)

Table 1. Summary of Nanodomain Properties of Various Receptors and Channels

Channel/receptor	Subcellular location	Diffusion coefficient (μm^2/s)	Nanodomain diameter (nm)	Nanodomain (kT)	Mean time of molecules in the nanodomain	Stability of the nanodomain
VGCC ($Ca_V2.1$) [13]	Presynaptic/axonal	$D_{well} = 0.086$	~80	3–4	~0.12 s (fourfold longer than free diffusion)	~30 s
Sodium channel ($Na_v1.6$) [95]	Somatic/dendritic	$D_{well} < 0.06$	~230	1.6 ± 0.7	>30 minutes	>30 minutes
AMPAR [27]	Postsynaptic/dendritic	$D_{spine} = 0.049$ $D_{shaft} = 0.13$ $D_{well} = 0.076$	200–400	3–6; some >8	Tens of seconds	A few minutes to tens of minutes
NMDAR [18]	Postsynaptic	$D_{GluN2A} = 0.001$ $D_{GluN2B} = 0.03^a$	10–100[b]	N.d.[c]	N.d.	N.d.
GlyR [42]	Postsynaptic/dendritic	$D_{well} = ~ 0.01$ $D_{dendrite} = 0.06$	200–300	3–4; some >6	1 s to tens of seconds	N.d.

[a]These data are from quantum dot labeled receptors and correspond to the colocalization with postsynaptic marker proteins.
[b]These data are based on localization microscopy data after fixation and do not take into account molecular fluctuations over time.
[c]N.d., not determined.

persist within the PSD for tens of minutes compared to 30 s for presynaptic VGCC nanodomains. To conclude, postsynaptic receptors are retained much longer in nanodomains, whereas presynaptic nanodomains of VGCCs are smaller and less stable (Figure 4 and Table 1).

Nanocolumn Organization Guarantees the Alignment of Pre- and Postsynaptic Nanodomains That Is Necessary for Optimal Synaptic Transmission

The **nanocolumn** concept [10,11] originates from the alignment of pre- and postsynaptic scaffold proteins, and proposes that VGCCs and receptors add to this structure to achieve an optimal configuration for SV release sites in the presynaptic terminal and the distribution of the receptors on the postsynaptic site. Indeed, the theory of diffusion in the synaptic cleft [48] reveals that these two distributions should be concentrated at one point and as aligned as far as possible. This was first anticipated numerically [8,9] for static receptor configurations and then for multiple columns [10] where, in addition, the concept was extended to trafficking receptors, showing that scaffold molecules should be concentrated at hotspots.

Comparing structures of scaffold proteins in the AZ and the PSD favored the idea of nanocolumns [11], and adhesion molecules are probably the core element of these proposed structures. However, several questions remain open: for example, how do such structures influence the probabilistic nature of synaptic transmission, and how stable is a nanocolumn? Proteolytic cleavage of adhesion molecules is an instructive mechanism to ensure a flexible subsynaptic rearrangement of trans-synaptic organization [15,96]. The mechanism of activity-dependent proteolytic cleavage of adhesion contacts and the flexible population of VGCCs and receptors in nanodomains question the exact role and reliability of nanocolumn alignment, and support the idea that synapse nanostructure is highly activity-dependent. Glial protrusions penetrating into the cleft could interfere with synaptic alignment and probably disturb this alignment [97], which could provide an additional example of fast changes in synaptic alignment. Another aspect

Figure 4. Schematic Representation of Pre- versus Postsynaptic Dynamic Organization. The presynaptic terminal contains multiple small Ca_V nanodomains (colored wells) with a lifetime of 30 s and a mean size of 80 nm. They can retain receptors for 120 ms. Few channels (3–10) can be retained in the same nanodomain. This calcium nanodomain can overlap with one or two docked vesicles (green) at most. Some of these nanodomains are apposed on the postsynaptic side to a cluster of AMPARs, forming a larger nanodomain with a size of a few hundreds of nanometers that is stable over minutes. This large nanodomain can retain receptors for seconds before they escape to the rest of the membrane. Ca_V and AMPAR nanodomains may form a nanocolumn alignment.

CellPress
REVIEWS

is alternative splicing, as exemplified here by VGCCs, but which is best known for adhesion molecules that impact on the nanoscale organization of synapses and their plasticity [98].

Multiple columns may function to isolate postsynaptic receptors from desensitization and allow different active units to be present in a single synapse [10]. However, the mechanism of nanocolumn alignment remains unclear. How many nanocolumns are needed, and where are they placed? Are nanocolumns present during synaptogenesis? What happens during synaptic plasticity? How stable are nanocolumns? Further investigations of the local arrangement of trans-synaptic interacting molecules during synaptic activity will help to clarify such questions, and may probably hint at strategies to interfere with synapse function by rearranging the molecular composition of a synapse rather than by blocking receptors or ion channels.

Concluding Remarks

Membrane nanodomains are not simply ensembles of proteins that aggregate. They are regions of high density that allow the circulation and retention of molecules. Nanodomains bring order to surface trafficking, driven by diffusion, a process that does not require ATP expenditure. Thus, the price to pay to use diffusion as the main driving force of motion with low targeting efficiency is compensated by the presence of nanodomains that retain receptors and channels in the right place (Figure 4).

A key characteristic of nanodomains is a structure that has low energy to keep receptors and channels in place. This low energy allows molecules to be bound for transient periods ranging from tens of milliseconds to tens of seconds. Such timescales are much longer than would be produced purely by diffusion, but are short enough to allow significant redistribution within the synapse. These molecular rearrangements maintain and adapt synaptic function in minimum time to modulate neuronal activity patterns and short-term plasticity.

Finally, we have defined nanodomains as regions where for example VGCCs and AMPARs can transiently enter and exit attracted by a field of force, not simply as aggregates. Thus, it is not clear whether these domains could be interpreted as phase separation [99]. In most cases these nanodomains are transients and should be able to change according to the demand for synaptic plasticity. Future work should reveal how synaptic nanodomains are generated and transformed or differ between populations of synapses, and this may call for refinement of the concept of transient phase separation.

References

1. Abbott, L.F. and Regehr, W.G. (2004) Synaptic computation. *Nature* 431, 796–803
2. Mi, Y. *et al.* (2017) Synaptic correlates of working memory capacity. *Neuron* 93, 323–330
3. Markram, H. *et al.* (1998) Differential signaling via the same axon of neocortical pyramidal neurons. *Proc. Natl. Acad. Sci. U. S. A.* 95, 5323–5328
4. Ermolyuk, Y.S. *et al.* (2012) Independent regulation of basal neurotransmitter release efficacy by variable Ca^{2+} influx and bouton size at small central synapses. *PLoS Biol.* 10, e1001396
5. Jensen, T.P. *et al.* (2019) Multiplex imaging relates quantal glutamate release to presynaptic Ca^{2+} homeostasis at multiple synapses in situ. *Nat. Commun.* 10, 1414
6. Le Duigou, C. *et al.* (2014) Recurrent synapses and circuits in the CA3 region of the hippocampus: an associative network. *Front. Cell. Neurosci.* 7, 262
7. Rolls, E.T. (2013) A quantitative theory of the functions of the hippocampal CA3 network in memory. *Front. Cell. Neurosci.* 7, 98
8. Xie, X. *et al.* (1997) Novel expression mechanism for synaptic potentiation: alignment of presynaptic release site and postsynaptic receptor. *Proc. Natl. Acad. Sci. U. S. A.* 94, 6983–6988
9. Raghavachari, S. and Lisman, J.E. (2004) Properties of quantal transmission at CA1 synapses. *J. Neurophysiol.* 92, 2456–2467
10. Freche, D. *et al.* (2011) Synapse geometry and receptor dynamics modulate synaptic strength. *PLoS One* 6, e25122

Outstanding Questions

What combination of individual interaction partners/scaffolds is crucial to allow flexible transient confinement of molecules such as receptors and ion channels at synapses?

What defines the residence time of molecules in pre- or postsynaptic nanodomains?

Are nanodomains organized similarly in inhibitory and excitatory synapses, and is the phase-separation framework well suited to describing them?

How are VGCC nanodomains reorganized following vesicle fusion?

How do multiple nanodomains (such as nanodomains associated with VGCCs, adhesion molecules, and SVs) overlap and interact?

How does nanodomain organization affect synaptic transmission, and can pre- and postsynaptic nanodomains autoregulate themselves?

How do nanodomains finely tune network rhythm, synchrony, or asynchronous release?

11. Tang, A.H. *et al.* (2016) A trans-synaptic nanocolumn aligns neurotransmitter release to receptors. *Nature* 536, 210–214

12. Nair, D. *et al.* (2013) Super-resolution imaging reveals that AMPA receptors inside synapses are dynamically organized in nanodomains regulated by PSD95. *J. Neurosci.* 33, 13204–13224

13. Heck, J. *et al.* (2019) Transient confinement of CaV2.1 Ca^{2+}-channel splice variants shapes synaptic short-term plasticity. *Neuron* 103, 66–79

14. Schneider, R. *et al.* (2015) Mobility of calcium channels in the presynaptic membrane. *Neuron* 86, 672–679

15. Trotter, J.H. *et al.* (2019) Synaptic neurexin-1 assembles into dynamically regulated active zone nanoclusters. *J. Cell Biol.* 218, 2677–2698

16. MacGillavry, H.D. *et al.* (2013) Nanoscale scaffolding domains within the postsynaptic density concentrate synaptic AMPA receptors. *Neuron* 78, 615–622

17. Crosby, K.C. *et al.* (2019) Nanoscale subsynaptic domains underlie the organization of the inhibitory synapse. *Cell Rep.* 26, 3284–3297

18. Kellermayer, B. *et al.* (2018) Differential nanoscale topography and functional role of GluN2–NMDA receptor subtypes at glutamatergic synapses. *Neuron* 100, 106–119

19. Hruska, M. *et al.* (2018) Synaptic nanomodules underlie the organization and plasticity of spine synapses. *Nat. Neurosci.* 21, 671–682

20. Dupuis, J.P. *et al.* (2014) Surface dynamics of GluN2B–NMDA receptors controls plasticity of maturing glutamate synapses. *EMBO J.* 33, 842–861

21. Penn, A.C. *et al.* (2017) Hippocampal LTP and contextual learning require surface diffusion of AMPA receptors. *Nature* 549, 384–388

22. Gramlich, M.W. and Klyachko, V.A. (2019) Nanoscale organization of vesicle release at central synapses. *Trends Neurosci.* 42, 425–437

23. Holcman, D. and Schuss, Z. (2015) Stochastic narrow escape in molecular and cellular biology. In *Analysis and Applications*, Springer, New York. [chapters 3-4]

24. Guerrier, C. and Holcman, D. (2018) The first 100 nm inside the pre-synaptic terminal where calcium diffusion triggers vesicular release. *Front. Synaptic Neurosci.* 10, 23

25. Byczkowicz, N. *et al.* (2018) How to maintain active zone integrity during high-frequency transmission. *Neurosci. Res.* 127, 61–69

26. Wu, M.M. *et al.* (2014) Single-molecule analysis of diffusion and trapping of STIM1 and Orai1 at endoplasmic reticulum–plasma membrane junctions. *Mol. Biol. Cell* 25, 3672–3685

27. Hoze, N. *et al.* (2012) Heterogeneity of AMPA receptor trafficking and molecular interactions revealed by superresolution analysis of live cell imaging. *Proc. Natl. Acad. Sci. U. S. A.* 109, 17052–17057

28. Chamma, I. *et al.* (2016) Mapping the dynamics and nanoscale organization of synaptic adhesion proteins using monomeric streptavidin. *Nat. Commun.* 7, 10773

29. Bademosi, A.T. *et al.* (2017) *In vivo* single-molecule imaging of syntaxin1A reveals polyphosphoinositide- and activity-dependent trapping in presynaptic nanoclusters. *Nat. Commun.* 8, 13660

30. Specht, C.G. *et al.* (2013) Quantitative nanoscopy of inhibitory synapses: counting gephyrin molecules and receptor binding sites. *Neuron* 79, 308–321

31. Fedchyshyn, M.J. and Wang, L.Y. (2005) Developmental transformation of the release modality at the calyx of Held synapse. *J. Neurosci.* 25, 4131–4140

32. Frischknecht, R. *et al.* (2009) Brain extracellular matrix affects AMPA receptor lateral mobility and short-term synaptic plasticity. *Nat. Neurosci.* 12, 897–904

33. Holcman, D. (2013) Unraveling novel features hidden in superresolution microscopy data. *Commun. Integr. Biol.* 6, e23893

34. Holcman, D. and Hoze, N. (2017) Statistical methods of short super-resolution stochastic single trajectories analysis. *Annu. Rev. Stat. Appl.* 4, 1–35

35. Holcman, D. *et al.* (2011) Narrow escape through a funnel and effective diffusion on a crowded membrane. *Phys. Rev. E Stat. Nonlinear Soft Matter Phys.* 84, 021906

36. Borgdorff, A.J. and Choquet, D. (2002) Regulation of AMPA receptor lateral movements. *Nature* 417, 649–653

37. Meier, J. *et al.* (2001) Fast and reversible trapping of surface glycine receptors by gephyrin. *Nat. Neurosci.* 4, 253–260

38. Dahan, M. *et al.* (2003) Diffusion dynamics of glycine receptors revealed by single-quantum dot tracking. *Science* 302, 442–445

39. Giannone, G. *et al.* (2010) Dynamic superresolution imaging of endogenous proteins on living cells at ultra-high density. *Biophys. J.* 99, 1303–1310

40. Manley, S. *et al.* (2008) High-density mapping of single-molecule trajectories with photoactivated localization microscopy. *Nat. Methods* 5, 155–157

41. Baumgart, F. *et al.* (2016) Varying label density allows artifact-free analysis of membrane-protein nanoclusters. *Nat. Methods* 13, 661–664

42. Masson, J.B. *et al.* (2014) Mapping the energy and diffusion landscapes of membrane proteins at the cell surface using high-density single-molecule imaging and Bayesian inference: application to the multiscale dynamics of glycine receptors in the neuronal membrane. *Biophys. J.* 106, 74–83

43. Hoze, N. and Holcman, D. (2015) Recovering a stochastic process from super-resolution noisy ensembles of single-particle trajectories. *Phys. Rev. E Stat. Nonlinear Soft Matter Phys.* 92, 052109

44. Schuss, Z. (1980) *Theory and Applications of Stochastic Differential Equations*, Wiley

45. Parutto, P. *et al.* (2019) Biophysics of high density nanometer regions extracted from super-resolution single particle trajectories: application to voltage-gated calcium channels and phospholipids. *Sci. Rep.* 9, 1–14

46. Holcman, D. and Schuss, Z. (2004) Escape through a small opening: receptor trafficking in the synaptic membrane. *J. Stat. Phys.* 117, 975–1014

47. Chandrasekhar, S. (1943) Stochastic problems in physics and astronomy. *Rev. Mod. Phys.* 15, 1–89

48. Taflia, A. and Holcman, D. (2011) Estimating the synaptic current in a multiconductance AMPA receptor model. *Biophys. J.* 101, 781–792

49. Petrini, E.M. *et al.* (2009) Endocytic trafficking and recycling maintain a pool of mobile surface AMPA receptors required for synaptic potentiation. *Neuron* 63, 92–105

50. Johnson, B. *et al.* (2018) Kv2 potassium channels form endoplasmic reticulum/plasma membrane junctions via interaction with VAPA and VAPB. *Proc. Natl. Acad. Sci. U. S. A.* 115, E7331–E7340

51. Kirmiz, M. *et al.* (2018) Remodeling neuronal ER–PM junctions is a conserved nonconducting function of Kv2 plasma membrane ion channels. *Mol. Biol. Cell* 29, 2410–2432

52. Matveev, V. *et al.* (2011) Calcium cooperativity of exocytosis as a measure of Ca^{2+} channel domain overlap. *Brain Res.* 1398, 126–138

53. Moreno, C.M. *et al.* (2016) Ca^{2+} entry into neurons is facilitated by cooperative gating of clustered CaV1.3 channels. *Elife* 5, e15744

54. Abbott, L.F. *et al.* (1997) Synaptic depression and cortical gain control. *Science* 275, 220–224

55. Fekete, A. *et al.* (2019) Underpinning heterogeneity in synaptic transmission by presynaptic ensembles of distinct morphological modules. *Nat. Commun.* 10, 826

56. Neef, J. *et al.* (2018) Quantitative optical nanophysiology of Ca^{2+} signaling at inner hair cell active zones. *Nat. Commun.* 9, 290

57. Nakamura, Y. *et al.* (2015) Nanoscale distribution of presynaptic Ca^{2+} channels and its impact on vesicular release during development. *Neuron* 85, 145–158

58. Rebola, N. *et al.* (2019) Distinct nanoscale calcium channel and synaptic vesicle topographies contribute to the diversity of synaptic function. *Neuron* 104, 693–710

59. Meinrenken, C.J. *et al.* (2002) Calcium secretion coupling at calyx of held governed by nonuniform channel-vesicle topography. *J. Neurosci.* 22, 1648–1667

60. Sheng, J. *et al.* (2012) Calcium-channel number critically influences synaptic strength and plasticity at the active zone. *Nat. Neurosci.* 15, 998–1006

61. Holcman, D. *et al.* (2018) Single particle trajectories reveal active endoplasmic reticulum luminal flow. *Nat. Cell Biol.* 20, 1118–1125

62. Sakamoto, H. *et al.* (2018) Synaptic weight set by Munc13-1 supramolecular assemblies. *Nat. Neurosci.* 21, 41–49

63. Neher, E. and Brose, N. (2018) Dynamically primed synaptic vesicle states: key to understand synaptic short-term plasticity. *Neuron* 100, 1283–1291

64. Delvendahl, I. *et al.* (2016) Fast, temperature-sensitive and clathrin-independent endocytosis at central synapses. *Neuron* 90, 492–498

65. Haucke, V. *et al.* (2011) Protein scaffolds in the coupling of synaptic exocytosis and endocytosis. *Nat. Rev. Neurosci.* 12, 127–138

66. Sieber, J.J. *et al.* (2007) Anatomy and dynamics of a supramolecular membrane protein cluster. *Science* 317, 1072–1076

67. Milovanovic, D. *et al.* (2015) Hydrophobic mismatch sorts SNARE proteins into distinct membrane domains. *Nat. Commun.* 6, 5984

68. Bornschein, G. *et al.* (2019) Neocortical high probability release sites are formed by distinct Ca^{2+} channel-to-release sensor topographies during development. *Cell Rep.* 28, 1410–1418

69. Miki, T. *et al.* (2017) Numbers of presynaptic Ca^{2+} channel clusters match those of functionally defined vesicular docking sites in single central synapses. *Proc. Natl. Acad. Sci. U. S. A.* 114, E5246–E5255

70. Holderith, N. *et al.* (2012) Release probability of hippocampal glutamatergic terminals scales with the size of the active zone. *Nat. Neurosci.* 15, 988–997

71. Vyleta, N.P. and Jonas, P. (2014) Loose coupling between Ca^{2+} channels and release sensors at a plastic hippocampal synapse. *Science* 343, 665–670

72. Brockmann, M.M. *et al.* (2019) RIM-BP2 primes synaptic vesicles via recruitment of Munc13-1 at hippocampal mossy fiber synapses. *Elife* 8, e43243

73. Eggermann, E. *et al.* (2012) Nanodomain coupling between Ca^{2+} channels and sensors of exocytosis at fast mammalian synapses. *Nat. Rev. Neurosci.* 13, 7–21

74. Keller, D. *et al.* (2015) An exclusion zone for Ca^{2+} channels around docked vesicles explains release control by multiple channels at a CNS synapse. *PLoS Comput. Biol.* 11, e1004253

75. Goswami, S.P. *et al.* (2012) Miniature IPSCs in hippocampal granule cells are triggered by voltage-gated Ca^{2+} channels via microdomain coupling. *J. Neurosci.* 32, 14294–14304

76. Williams, C. *et al.* (2012) Coactivation of multiple tightly coupled calcium channels triggers spontaneous release of GABA. *Nat. Neurosci.* 15, 1195–1197

77. Ermolyuk, Y.S. *et al.* (2013) Differential triggering of spontaneous glutamate release by P/Q-, N- and R-type Ca^{2+} channels. *Nat. Neurosci.* 16, 1754–1763

78. Chanaday, N.L. *et al.* (2019) The synaptic vesicle cycle revisited: new insights into the modes and mechanisms. *J. Neurosci.* 39, 8209–8216

79. Biederer, T. *et al.* (2017) Transcellular nanoalignment of synaptic function. *Neuron* 96, 680–696

80. Korber, C. and Kuner, T. (2016) Molecular machines regulating the release probability of synaptic vesicles at the active zone. *Front. Synaptic Neurosci.* 8, 5

81. Choquet, D. (2018) Linking nanoscale dynamics of AMPA receptor organization to plasticity of excitatory synapses and learning. *J. Neurosci.* 38, 9318–9329

82. Bats, C. *et al.* (2007) The interaction between stargazin and PSD-95 regulates AMPA receptor surface trafficking. *Neuron* 53, 719–734

83. Opazo, P. *et al.* (2010) CaMKII triggers the diffusional trapping of surface AMPARs through phosphorylation of stargazin. *Neuron* 67, 239–252

84. Daw, M.I. *et al.* (2000) PDZ proteins interacting with C-terminal GluR2/3 are involved in a PKC-dependent regulation of AMPA receptors at hippocampal synapses. *Neuron* 28, 873–886

85. Rouach, N. *et al.* (2005) TARP gamma-8 controls hippocampal AMPA receptor number, distribution and synaptic plasticity. *Nat. Neurosci.* 8, 1525–1533

86. von Engelhardt, J. *et al.* (2010) CKAMP44: a brain-specific protein attenuating short-term synaptic plasticity in the dentate gyrus. *Science* 327, 1518–1522

87. Schwenk, J. *et al.* (2014) Regional diversity and developmental dynamics of the AMPA-receptor proteome in the mammalian brain. *Neuron* 84, 41–54

88. Klaassen, R.V. *et al.* (2016) Shisa6 traps AMPA receptors at postsynaptic sites and prevents their desensitization during synaptic activity. *Nat. Commun.* 7, 10682

89. Kato, A.S. *et al.* (2008) AMPA receptor subunit-specific regulation by a distinct family of type II TARPs. *Neuron* 59, 986–996

90. Ehlers, M.D. *et al.* (2007) Diffusional trapping of GluR1 AMPA receptors by input-specific synaptic activity. *Neuron* 54, 447–460

91. Heine, M. *et al.* (2008) Surface mobility of postsynaptic AMPARs tunes synaptic transmission. *Science* 320, 201–205

92. Xiao, M.Y. *et al.* (2004) Creation of AMPA-silent synapses in the neonatal hippocampus. *Nat. Neurosci.* 7, 236–243

93. Franks, K.M. *et al.* (2003) Independent sources of quantal variability at single glutamatergic synapses. *J. Neurosci.* 23, 3186–3195

94. Chen, X. *et al.* (2015) PSD-95 family MAGUKs are essential for anchoring AMPA and NMDA receptor complexes at the postsynaptic density. *Proc. Natl. Acad. Sci. U. S. A.* 112, E6983–E6992

95. Akin, E.J. *et al.* (2016) Single-molecule imaging of Nav1.6 on the surface of hippocampal neurons reveals somatic nanoclusters. *Biophys. J.* 111, 1235–1247

96. Peixoto, R.T. *et al.* (2012) Transsynaptic signaling by activity-dependent cleavage of neuroligin-1. *Neuron* 76, 396–409

97. Pannasch, U. *et al.* (2014) Connexin 30 sets synaptic strength by controlling astroglial synapse invasion. *Nat. Neurosci.* 17, 549–558

98. Furlanis, E. and Scheiffele, P. (2018) Regulation of neuronal differentiation, function, and plasticity by alternative splicing. *Annu. Rev. Cell Dev. Biol.* 34, 451–469

99. Feng, Z. *et al.* (2019) Phase separation as a mechanism for assembling dynamic postsynaptic density signalling complexes. *Curr. Opin. Neurobiol.* 57, 1–8

100. Balzarotti, F. *et al.* (2017) Nanometer resolution imaging and tracking of fluorescent molecules with minimal photon fluxes. *Science* 355, 606–612

101. Taylor, R.W. *et al.* (2019) Interferometric scattering microscopy reveals microsecond nanoscopic protein motion on a live cell membrane. *Nat. Photonics* 13, 480–487